

## A Survey of Techniques for the Display of Continuous Tone Pictures on Bilevel Displays

J. F. JARVIS, C. N. JUDICE, AND W. H. NINKE

Bell Laboratories, Holmdel, New Jersey 07733

Communicated by Leon D. Harmon

Received June 13, 1975

Many displays are basically bilevel in nature with individual display cells, all of the same size, arranged in a rectangular array. We present a survey of processing techniques for presenting continuous tone still images on such displays. Four techniques are covered in detail while several others are covered briefly. All the techniques achieve the subjective effect of continuous tone by properly controlling only the spatial density of bilevel display states.

The processing techniques consist of dividing an image into picture elements and comparing the intensity of each element with a threshold value. If the element intensity is greater than the threshold, the corresponding display cell is set to the bright state; otherwise, the cell is set to the dark state. In the *ordered-dither* technique, the threshold is spatially dependent, i.e., it is determined only by the coordinates of the element being processed. In the remaining three techniques, *constrained average*, *dynamic threshold*, and *minimized average error*, the threshold is determined by values of elements close to the one currently being processed. The latter three thus require more processing and more storage than the first, but allow some edge emphasis. Images processed by all the described techniques are exhibited.

### 1. INTRODUCTION

Many display and recording media are basically bilevel in nature. Individual display cells or sites are either on or off, bright or dark, white or black, reflective or absorptive, etc. Liquid crystal displays, ac-sustained gas discharge or plasma panels, microfilm recorders, and ink on paper all fall in this category. In this survey paper we present a family of processing techniques for presenting continuous tone still images on bilevel displays. The images may be real scenes originated from a camera or film scanner, or may be computer-composed. All the techniques achieve the subjective effect of continuous tone by properly controlling only the spatial density of bilevel display states.

Our examination of various techniques was motivated by our desire to use ac plasma panels in a direct-view two-way image communication system. The techniques we discuss, however, were collected from a wide variety of literature and are, of course, not limited to our system goals. They are applicable to many

areas including facsimile transmission, computer-aided instruction, simulation display, computer-produced movies, medical instrumentation, and others.

We have chosen to concentrate on the techniques that give the best displayed images and, because we are interested in inherent memory displays, have not accepted constraints on storage such as would be required for a refreshed display of a processed picture [1]. We have, however, set some guidelines, to be detailed shortly, to ensure that a technique has potential for simple hardware implementation. Additional constraints met by the techniques we present are that the spatial resolution of the display be the same as the sampling resolution of the original image and that the final display media be bilevel with individual display cells, all of the same size, arranged in a rectangular array. Thus, our survey differs from a previous one [2] that described techniques in which a number of bilevel cells are used to form one image element. What we describe also differs from efforts with gas discharge displays using multiple stable cell states [3], from a number of ac gas panel "TV" efforts where time and space division techniques [4-6] have been used in an attempt to present continuous tone representations with dynamic scenes, and from newspaper halftone schemes where display cell size varies. We concentrate on representing still images as a collection of bilevel states of cells of a display. If the display has inherent memory, individual cells are set once and left as set for the time that the image display is desired. If the display has no memory but must be refreshed periodically to prevent flicker, the cells are always set during a refresh cycle to the status originally selected to present the image.

## 2. ALGORITHMS FOR THE REDUCTION OF A CONTINUOUS TONE IMAGE TO A BILEVEL REPRESENTATION

The basic processing organization to produce the drive signal for a bilevel display is shown in Fig. 1. An image is divided into picture elements (pel's) and the multibit signal representing each picture element intensity is compared with a threshold signal. If the image intensity is greater than the threshold, the corresponding display cell is set to the bright state; otherwise, the cell is set to the dark state. Although digital signals and a digital comparator are shown, analog signals and an analog comparator could similarly be used. The processing algorithms we describe differ primarily in the way they produce the threshold values for comparison with the picture elements intensities.

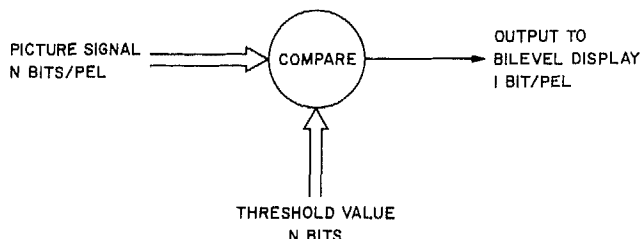


FIG. 1. Basic processing method for simulating continuous tone pictures on bilevel displays.

In the remainder of this section we first describe and then dismiss several obvious ways of choosing threshold values on the grounds that poor-quality displayed images are produced. We then describe in detail four processing algorithms that produce good images and exhibit images processed by them. The first algorithm, ordered dither, uses a simple set of threshold values that are unaffected by image values. The remaining three use image values in the neighborhood of a picture element to determine the threshold value to be used for that picture element. The latter three thus require more storage and more processing than the first.

Many algorithms of the latter type are possible. The ones we present should possess efficient hardware implementations because we have imposed several restrictions on them. The first is that the algorithm not require any parameters obtainable only by a prior scan of the entire picture. Alternatively stated, the decision to turn on a particular cell is made only on the basis of information local to the pel being considered. A second restriction is that the algorithms be completely deterministic. That is, once a decision is made on a pel, no further processing can change its state. The third general restriction is that the algorithms be capable of accepting the source data sequentially, elements along a line and lines within a frame.

### *2.1 Notations and Conventions*

To simplify the algorithm presentations and maintain as much coherence as practical, the following notation will be used in each description. A frame is defined as a set of  $N^2$  samples taken on a square geometric grid of  $N$  lines with  $N$  samples per line. For the implementation described in this paper,  $N = 512$ . Each of the  $N^2$  samples,  $I_{xy}$ , is an image intensity value quantized to eight bits. The subscripts  $x$  and  $y$  label the positions within a line, and lines within a frame, respectively. The subscripts are in the range 0 to  $N - 1$ . Black is represented by  $I_{xy} = 0$  and white by  $I_{xy} = R$ , where  $R$  is the maximum value possible ( $R = 255$  in our implementations, corresponding to the eight-bit intensity quantization). Each algorithm produces a displayed intensity  $P_{xy}$  corresponding to input value,  $I_{xy}$ . Intensity  $P_{xy}$  can have value  $R$  or 0 corresponding to the two possible display conditions, on or off.

In the discussion of individual processing techniques the presentation will consist of a concise statement of the processing followed by a discussion of parameters used and some brief comments on the implementation requirements. Figures illustrating the processing are photographs of an Owens-Illinois 512-60 DIGIVUE panel. Figures are grouped by the same original image. This will cause some jumping around when looking at one kind of processing on different subject images but facilitates comparison of different processing for the same subject.

### *2.2 Some Obvious Processing Techniques*

A number of picture processing algorithms were examined and not considered suitable for a variety of reasons, primarily the quality of output image.



FIG. 2. Face, photographic original.



FIG. 3. Face, processed with an  $8 \times 8$  dither matrix.



FIG. 4. Face, processed by the constrained average method.



FIG. 5. Face, processed by the constrained average method with a dither signal added.



FIG. 6. Face, processed by the dynamic threshold method.



FIG. 7. Face, processed by the minimized average error method.



FIG. 8. Face, processed with a fixed threshold of 150.



FIG. 9. Face, processed with a random threshold.



FIG. 10. Face, processed with the equalized histogram dither matrix.



FIG. 11. Face, 256 × 256 pels displayed using four cells/pel.



FIG. 12. Face,  $256 \times 256$  pels, interpolated to  $512 \times 512$  and processed with an  $8 \times 8$  dither matrix.



FIG. 13. Face, processed with a  $16 \times 16$  matrix containing each value, 0-255, once and with the element locations specified at random.

The fixed threshold technique is the simplest to implement in that the decision rule is simply stated:

$$\text{If } I_{xy} > T, \quad \text{then } P_{xy} = R, \\ \text{else } P_{xy} = 0. \quad (1)$$

The threshold  $T$  is usually in the neighborhood of  $R/2$ . Often, a high-contrast text or line image can be successfully displayed by this technique; however, continuous tone subjects generate output images consisting of featureless bands of lit cells that bear only an outline resemblance (see Fig. 8) to the original (see Fig. 2). A threshold,  $T = 150$ , was used to produce Fig. 8.

A slight improvement over the fixed threshold is to replace  $T$  by equally distributed random numbers over the range 0 to  $R$  with a new random number generated for each  $I_{xy}$ . The resulting image now shows obvious tonal variations but suffers from large amounts of noise and poor resolution (see Fig. 9). The discussion on dither (Section 2.3) will indicate why this is so.

A further group of techniques rejected as unsatisfactory arises when there are  $n$  display elements ( $n > 1$ ) available for each source sample,  $I_{xy}$ . Under this condition,  $n + 1$  discrete intensities are possible by lighting the appropriate number of cells as a function of the image intensity,  $I_{xy}$ . When  $n$  is small ( $n < 16$ ), objectional contouring results. Figure 11 shows processing with four cells/pel. There is also a substantial loss of resolution as  $n$  gets larger. By employing different patterns for the intermediate brightness levels, contouring can be reduced at the expense of added spatial noise.

### 2.3 Ordered Dither

The ordered-dither [7-10] technique generates a bilevel representation of continuous tone images by comparing the image values,  $I_{xy}$ , to a position-dependent set of thresholds. The set of thresholds is contained in the  $n \times n$  dither matrix  $D^n$  with the choice of matrix element values and their arrangement in the matrix being the key to the dither technique. For an  $n \times n$  matrix,  $D^n$ , dithering is accomplished as follows. A matrix element  $D^n_{ij}$  is selected from the coordinate of the point being evaluated:

$$\begin{aligned} i &= x \text{ modulo } n, \\ j &= y \text{ modulo } n. \end{aligned} \quad (2)$$

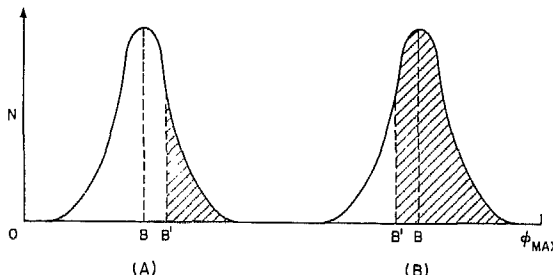


FIG. 14. Relationship at threshold to average brightness for the constrained average processing method.

0	32	64	96	128	160	192	224
8							
16							
24	56						248
0-255 ALTERNATE VERTICAL LINES, 224 AND 32							
64 0-255 AND 255-0 HORIZONTAL LINES							
128							
192							

FIG. 15. A map describing the contents of the computer-generated file used to make Figs. 26-30. The top four rows are patches of constant intensities. The next row is an intensity ramp varying from 0 on the left to 255 at the right. Alternate vertical lines in this area have intensities of 224 and 32. The bottom three rows are constant intensities with horizontal lines varying from minimum to maximum brightness.

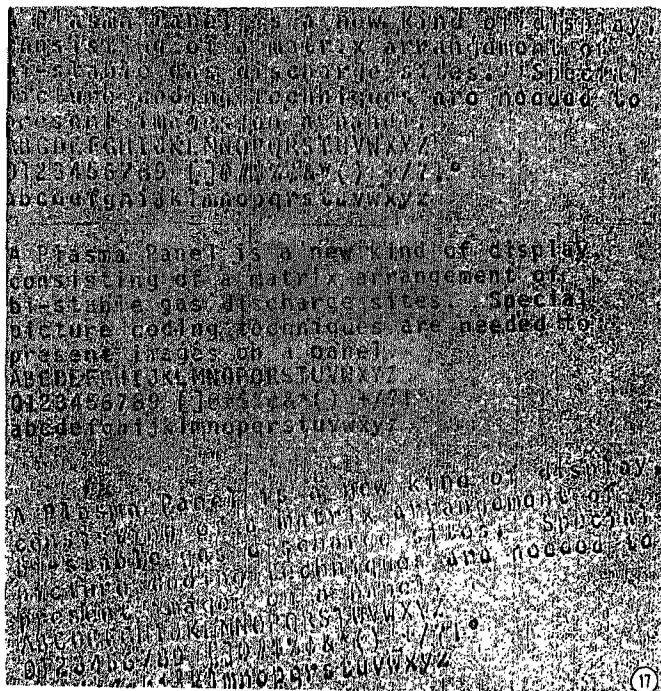
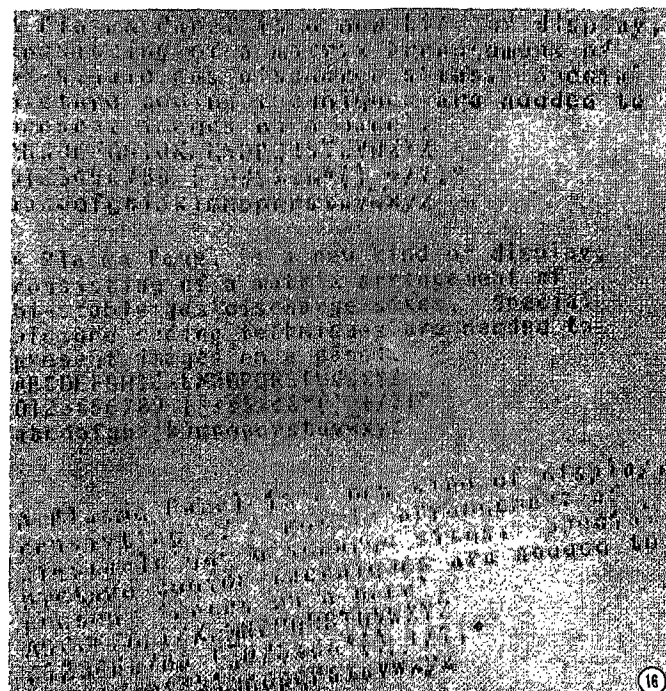
The decision to light cell  $x,y$  is then:

$$\text{If } I_{xy} > D^n_{ij}, \quad \text{then } P_{xy} = R, \\ \text{else } P_{xy} = 0. \quad (3)$$

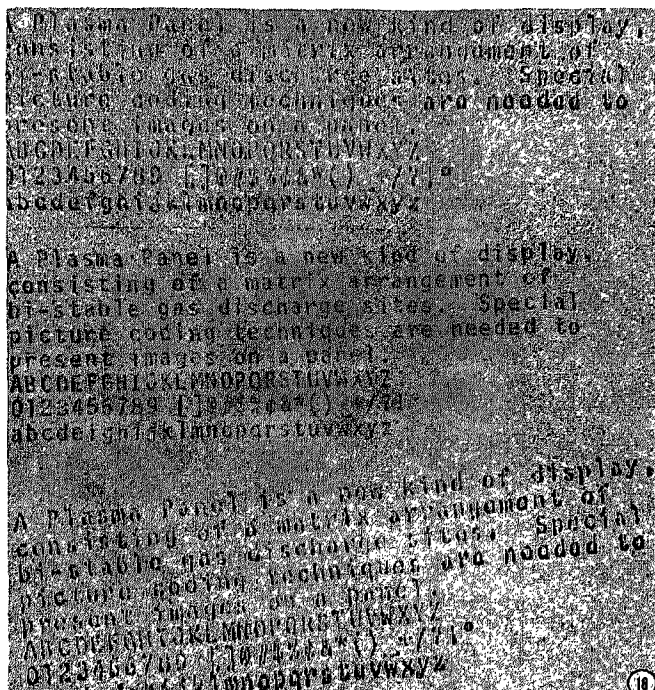
The matrix element selection rule (2) causes the dither matrix to be repeated in checkerboard fashion over the entire source image. The key to this technique is, of course, the contents of the dither matrix,  $D^n$ .

Historically, ordered dither was first proposed by Limb [7] as a means of reducing contouring in TV images reproduced with a limited number of intensity levels. The dither patterns used were determined from evaluation of a visual model and confirmed by subjective tests. This technique was later applied to bilevel representations of continuous tone pictures by Lippel and Kurland [8]. An optimization criterion was proposed by Bayer [9] and used to generate dither patterns that do not introduce much low spatial frequency noise into a displayed image. Visually, this means that the patterns do not introduce texture in the display of a picture with low detail and relatively constant brightness. In our previous paper [10] on dither techniques we exhibited a recursion relationship between the  $2 \times 2$  matrix of Limb and the matrices generated by Bayer. Given that

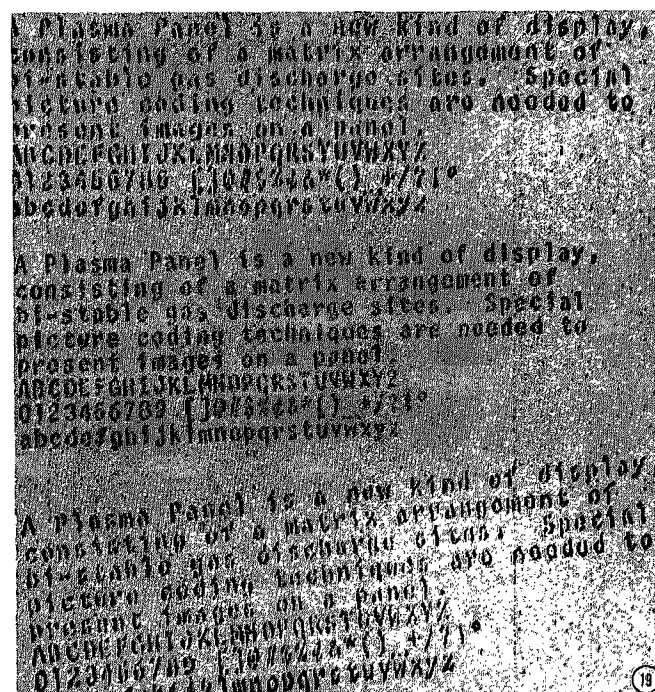
$$D^2 = \begin{vmatrix} 0 & 2 \\ 3 & 1 \end{vmatrix} \quad (4)$$



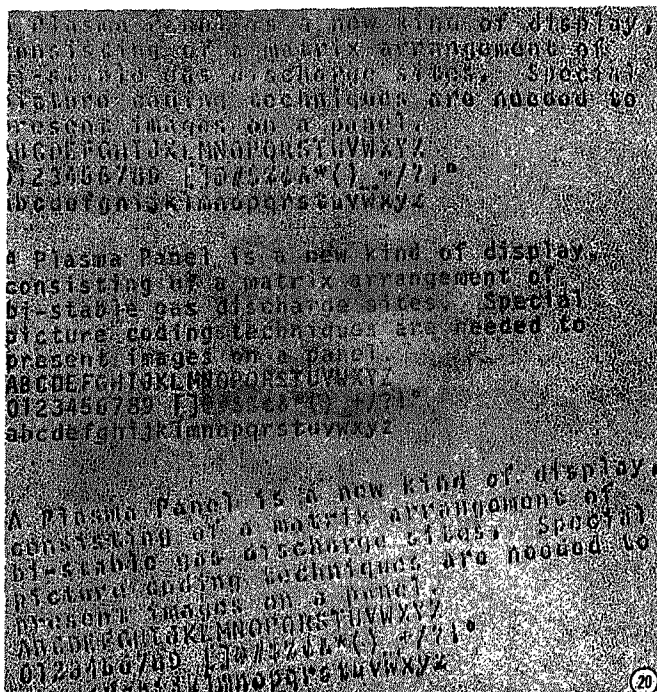
Figs. 16-20. The figures are of a sample of typewritten text. The processing is the same as in Figs. 3-7, respectively.



(18)



(19)



and defining

$$U^n = \begin{vmatrix} 1 & 1 \cdots 1 \\ 1 & 1 \cdots 1 \\ \vdots & \vdots \\ 1 & \end{vmatrix} \quad (5)$$

allows the statement of the recursion relationship as

$$D^n = \begin{vmatrix} 4D^{n/2} + D^2_{00}U^{n/2} & 4D^{n/2} + D^2_{01}U^{n/2} \\ 4D^{n/2} + D^2_{10}U^{n/2} & 4D^{n/2} + D^2_{11}U^{n/2} \end{vmatrix}. \quad (6)$$

Equation (4) is one of four possible  $2 \times 2$  matrices that satisfy the Bayer optimization criterion. The first recursion produces the  $4 \times 4$  matrix,  $D^4$ :

$$D^4 = \begin{vmatrix} 0 & 8 & 2 & 10 \\ 12 & 4 & 14 & 6 \\ 3 & 11 & 1 & 9 \\ 15 & 7 & 13 & 5 \end{vmatrix}. \quad (7)$$

Several properties of dithering can be seen by examining Eqs. (6) and (7). First,  $n^2 + 1$  discrete intensities can be reproduced by a matrix  $D^n$ , as the elements include each integer value from 0 to  $n^2 - 1$  exactly once. The displayed image does not lose spatial resolution as  $n$  is increased, even though the intensity resolution increases. The recursive nature of the generation allows any  $D^n$  to be reproduced from an appropriate combination of submatrices,  $aD^2 + bU^2$ , where

the coefficients  $a$  and  $b$  follow from the order of  $D^n$ . Since the matrix  $D^2$  will show intensity gradients greater than  $R/8$ , the larger matrices will still display gradients of this magnitude over the same distances. These considerations are explored more fully in the authors' paper [10] on the dither technique.

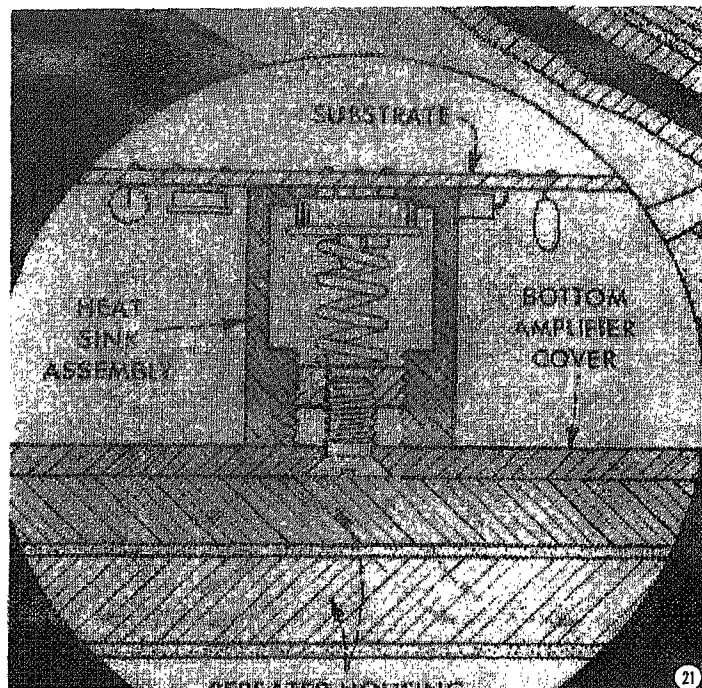
Figures 3, 16, 21, and 26 show dithering applied to the  $512 \times 512$  pel data files and displayed on an ac plasma panel. The matrix  $D^8$  was used for these figures. The smaller matrices tend to show contouring, while  $D^{16}$  does not generate a noticeably different output from the matrix  $D^8$ . The latter result is not too surprising, as  $D^{16}$  consists of four submatrices  $D^8$  differing from each other by 1. Since the source data noise is greater than 4 intensity units, the additional fineness in the thresholds in  $D^{16}$  does not produce a significant difference in the output image. When matrices smaller than  $D^{16}$  were used, an appropriate scaling factor was used so the matrix elements were equally spaced in the 0–255 range. A variation on this approach is to space the matrix elements in the dither matrix such that each subjective intensity in the processed picture has an equal probability of occurring. This process, called the equalized intensity histogram algorithm, is a nonlinear mapping of the source to displayed intensity. For the image of the face the processing result is excellent (Fig. 10); however, processing images containing large areas of constant intensity causes the resulting image to have substantial amounts of undesired texture in those nominally constant intensity areas. Since the adjusted dither matrix is based on the total intensity distribution of the source picture this technique also fails to meet the requirement of only using processing local to the pel being evaluated.

The importance of the spatial arrangement of the matrix elements of the dither matrix on the displayed image is clearly shown by generating a  $16 \times 16$  matrix containing each element value between 0 and 255 with the element positions specified at random. The  $16 \times 16$  matrix is clearly visible in Fig. 13, showing that ignoring the criteria of minimizing lower spatial frequency errors results in a poor rendition.

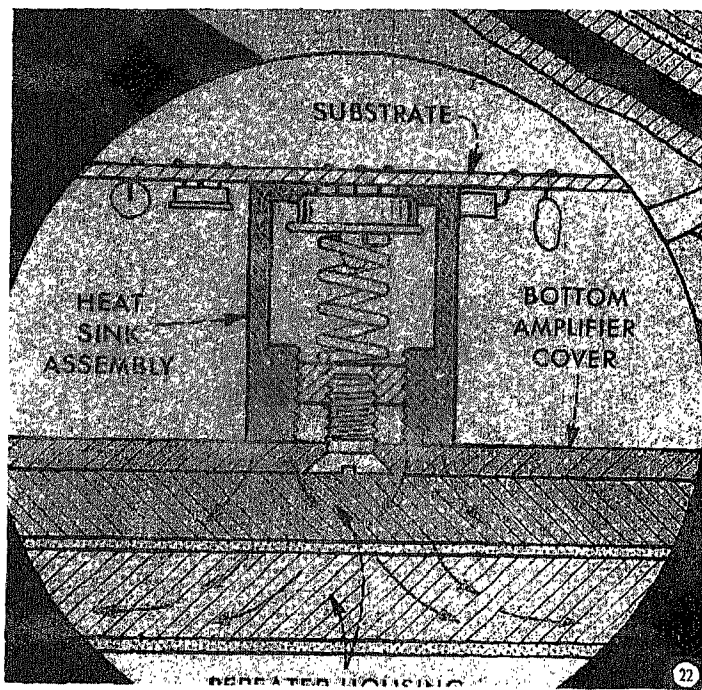
The question arises whether ordered dither or a number of display cells per original picture element, as mentioned before, should be used if the display resolution is greater than the original image resolution. We have found, in general, that images with less resolution than the display seem to be best reproduced when the images are interpolated to have a resolution equal to the display resolution and ordered dither is used. For example, a picture  $S$ , coded as  $256 \times 256$  samples, is used to generate a  $512 \times 512$  element picture by

$$\begin{aligned} I_{xy} &= S_{x'y'}, \\ I_{x+1,y} &= \frac{1}{2}(S_{x'y'} + S_{x'+1,y'}), \\ I_{x,y+1} &= \frac{1}{2}(S_{x'y'} + S_{x',y'+1}), \\ I_{x+1,y+1} &= \frac{1}{4}(S_{x'y'} + S_{x'+1,y'} + S_{x',y'+1} + S_{x'+1,y'+1}), \end{aligned} \quad (8)$$

where  $x = 2x'$  and  $y = 2y'$ . Although there is no gain in resolution from this interpolation the picture quality is substantially better than obtained by simply using four cells for each pel. Figure 12 shows the same data as used in Fig. 11 after interpolation to a  $512 \times 512$  grid and processing by the dither technique.

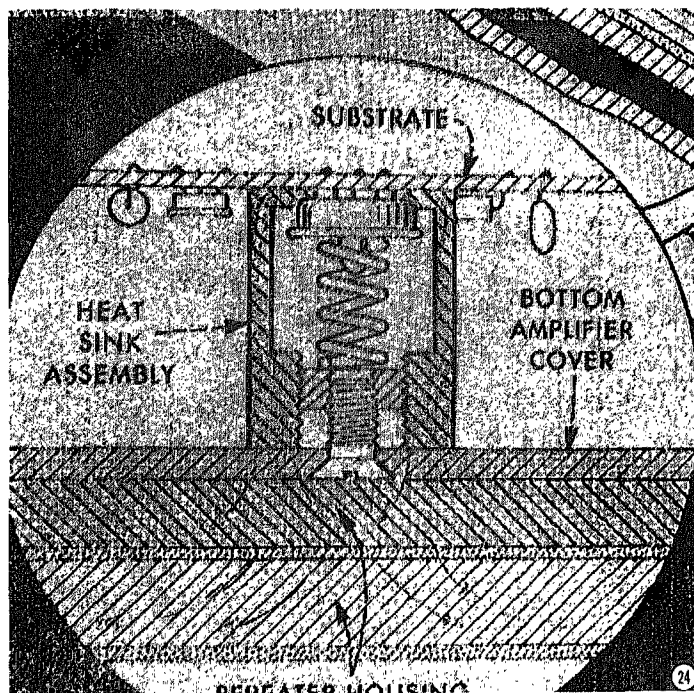
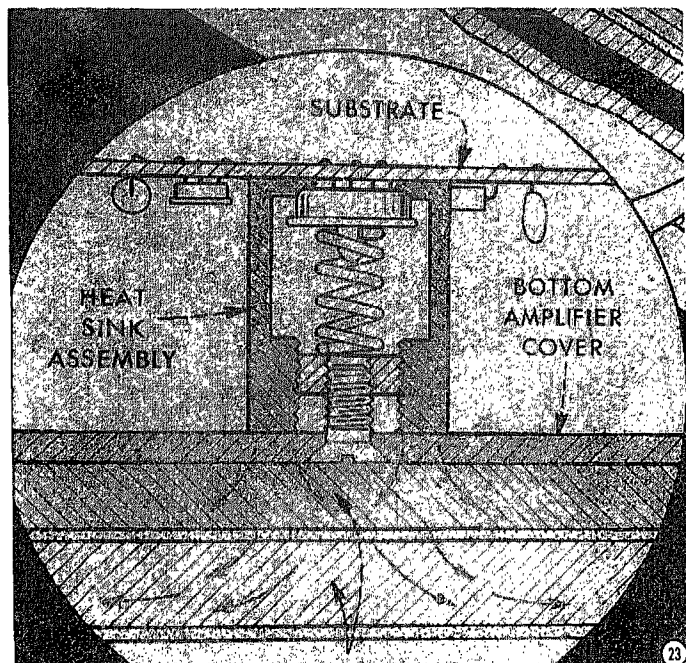


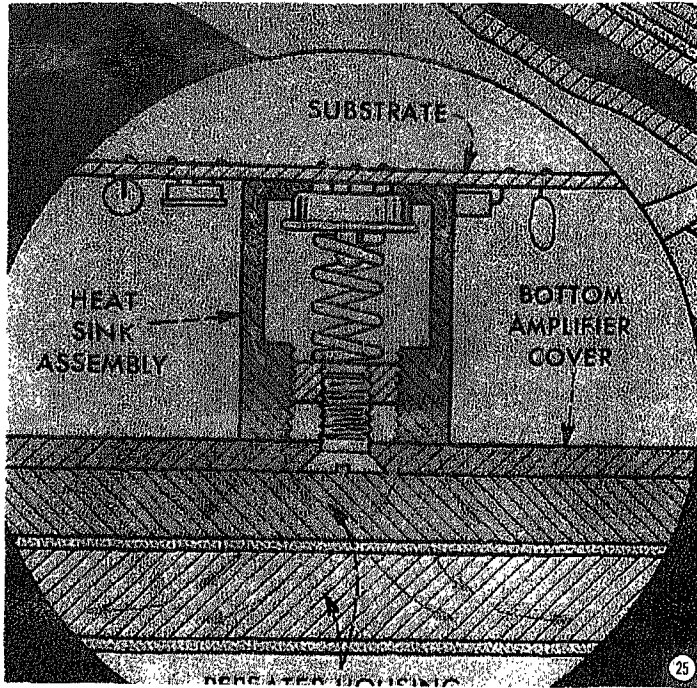
(21)



(22)

Figs. 21-25. These figures are a portion of a drawing. The processing is the same as in Figs. 3-7, respectively.





Implementation of ordered dither can be made with a read-only memory to contain or specialized logic to generate the dither matrix and a comparison operator. No auxiliary memory is needed for image data. Since the dither matrix will be a power of 2 in size, the modulo operation in Eq. (2) can be accomplished by taking the low bits of the  $x$  and  $y$  position registers.

#### 2.4 Constrained Average

This technique [11] combines edge emphasis and gray scale rendition in a single process. Edge emphasis creates an enhanced legibility of textual, line and other material of high detail, while gray scale rendition is necessary to display continuous tone original images properly. The processing, through the comparison of the intensity at a point with an average intensity computed in the immediate neighborhood of the point, provides edge emphasis capability. The comparison process also gives gray scale by using the finite signal/noise ratio for the picture data being processed to provide, on a statistical basis, a number of lit cells related to the average image intensity in a picture area.

The on or off decision for the cell,  $I_{xy}$ , is reached by the following steps. First, the average intensity,  $B_{xy}$ , in the neighborhood of  $I_{xy}$  is calculated. This can be done either by an explicit sum over  $I_{xy}$  and its nearest neighbors or by the appropriate digital low-pass filter. Next, a threshold  $B'$  is computed from the relationship

$$B'_{xy} = \gamma + [1 - (2\gamma/R)]B_{xy}, \quad (9)$$

which linearly maps  $B_{xy}$ ,  $0 \leq B_{xy} \leq R$ , into  $B'_{xy}$ , where  $\gamma \leq B'_{xy} \leq R - \gamma$ .

This parameter  $\gamma$  controls the apparent contrast of the output image and  $\gamma \neq 0$  is required to produce a gray scale in the output image. The meaning of  $\gamma$  will be discussed more fully in following paragraphs. Finally, the decision is made on lighting cell  $xy$ :

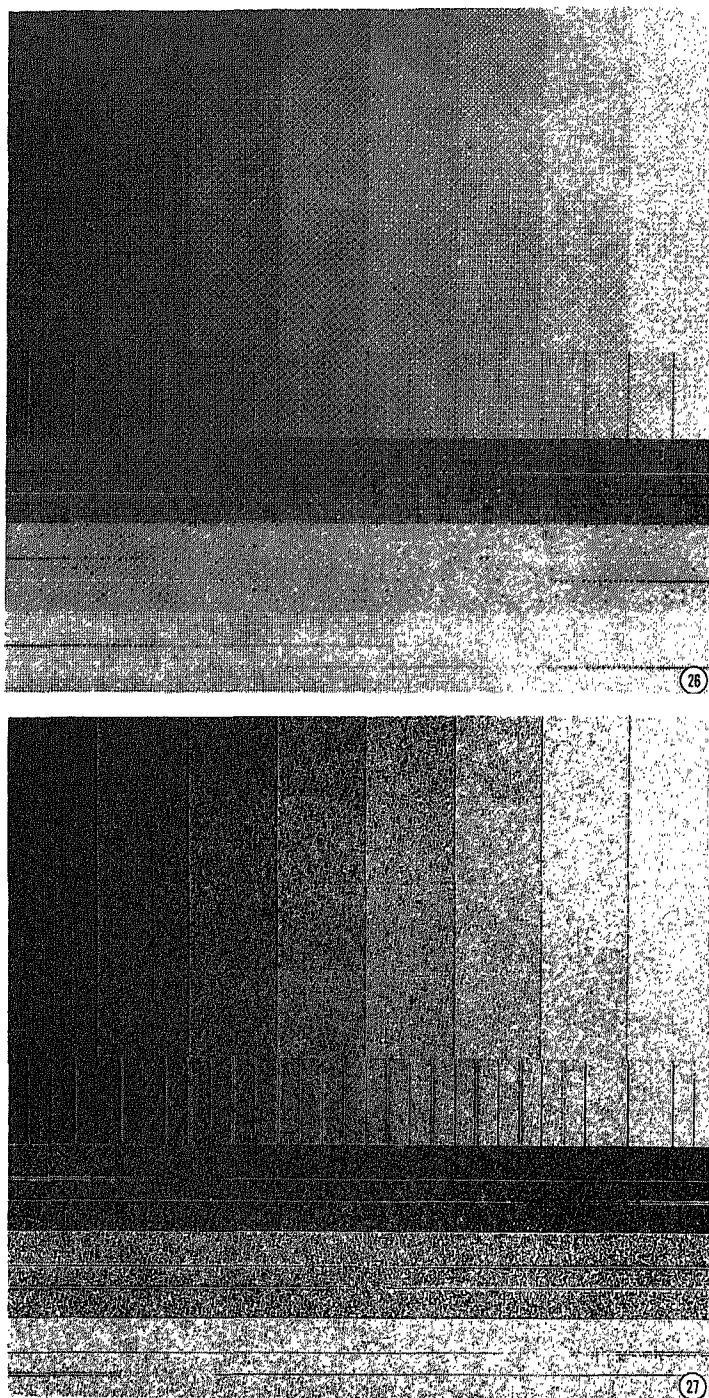
$$\begin{aligned} \text{If } I_{xy} > B'_{xy}, \quad & \text{then } P_{xy} = R, \\ \text{else } P_{xy} = 0. \end{aligned} \quad (10)$$

The claim was made that this processing provides adequate rendition of continuous tone images and edge emphasis. Edge emphasis is achieved as any cell differing markedly from the average will be forced on or off depending on its relationship to the average. This is certainly obvious in the case of  $\gamma = 0$  and since small  $\gamma$  ( $\gamma < R/10$ ) are used to produce the gray scale, the qualitative result of edge emphasis is not changed.

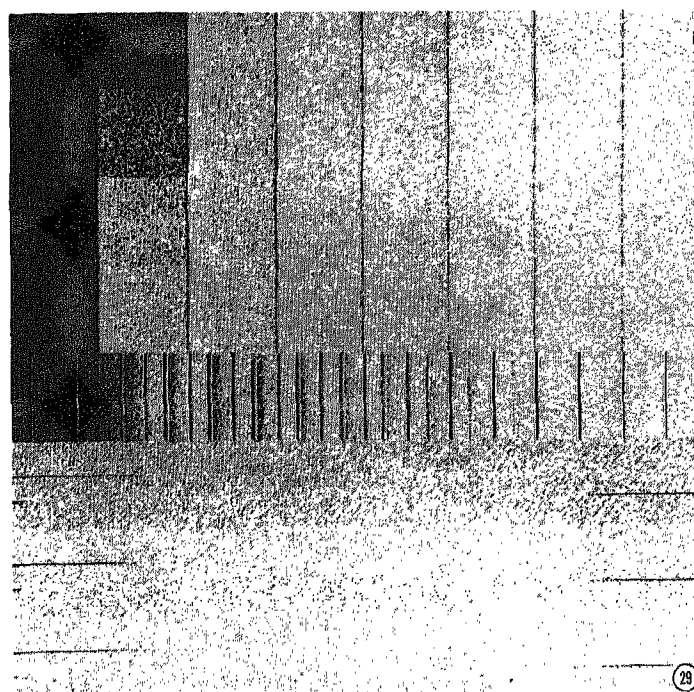
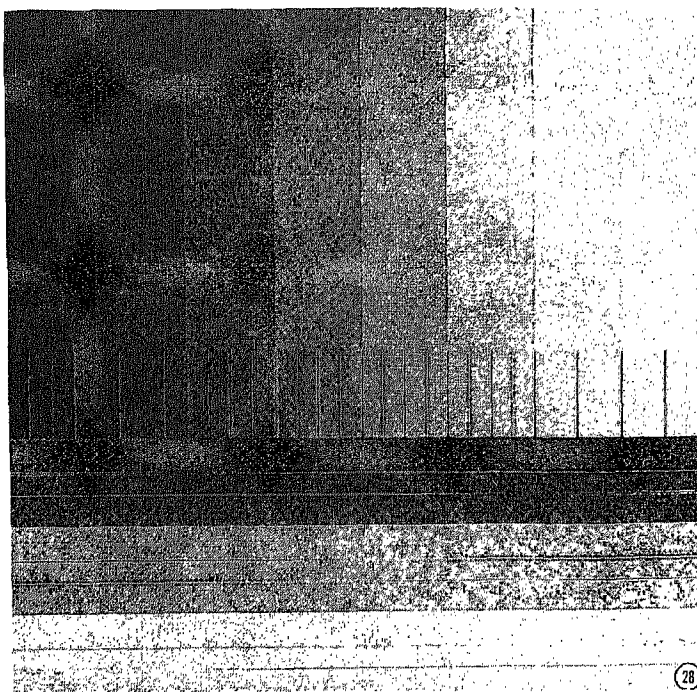
The explanation of how the gray scale is obtained is somewhat more complicated. A qualitative description will be given here and if a more thorough treatment is desired the reader is referred to Ref. [11], which contains a detailed analysis assuming rectangular and Gaussian noise statistics on the picture signal. To visualize how the gray scale is obtained, consider an image area of constant brightness. Since the picture data signal to noise ratio ( $S/N$ ) is finite there will be a distribution of intensity values for this nominally constant intensity region. The average,  $B$ , will also show a distribution but it will be narrower as the noise component in each pel is uncorrelated. By Eq. (9),  $B' < B$  for  $B > R/2$  and  $B' > B$  for  $B < R/2$ , and since  $B'$  is used as the decision threshold, the following result is obtained. In areas of average intensity greater than  $R/2$  more than one-half of the cells on the average will be lit as  $B' < B$  (Fig. 14A). In the opposite case, when the average brightness is less than  $R/2$ , fewer than one-half of the cells will be on as  $B' > B$  (Fig. 14B). As the average brightness approaches the extremes, a vanishingly small number will be on or off if  $\gamma$  is chosen somewhat larger than the noise amplitude. For the processing results shown in this paper the local average was computed from  $I_{xy}$  and its eight nearest neighbors in the picture by a simple summing operation.

Since the inherent noise in the data generates the detailed dot patterns, the resulting picture has a grainy or noisy appearance (Figs. 4, 17, 22, 27). Also, the effective contrast depends on the data  $S/N$  with a lower apparent contrast achieved for a smaller  $S/N$  and a fixed  $\gamma$ . Both of these problems can be alleviated by adding a dither signal to the data with an amplitude greater than the data noise amplitude. In particular, if the added signal is a position-dependent dither pattern the resulting bilevel picture will have a detailed dot pattern that tends to show the regular dither pattern (Figs. 5, 18, 23, 28). When the peak-to-peak dither amplitude is greater than  $2\gamma$  and  $\gamma$  is greater than the signal/noise amplitude, the full gray scale is reproduced by the dither pattern and the optimum  $\gamma$  is no longer dependent on the data  $S/N$ . The added dither pattern does not affect the edge emphasis, which becomes clearly apparent as the detail structure exceeds  $\gamma$  in amplitude.

In the processing of the data in Figs. 4, 17, 22, and 28, a value of  $\gamma = 10$  was used. This value was arrived at subjectively as the one that best reproduced the



Figs. 26-30. These figures are made from the computer-generated file described in Fig. 15. The processing is the same as in Figs. 3-7, respectively.





three photographically obtained images. In the processing of the combined constrained average and dither algorithms a 10% amplitude (-12 to +12 range) dither signal was added and  $\gamma = 20$  was used. Again the choice of parameters was subjectively made on the basis of the three photographic test subjects.

Implementation, as described, requires three line memories to provide data needed to compute the neighborhood average. The neighborhood average also requires either a low-pass digital filter or a number of adders, depending on the computation technique. Assuming a fixed  $\gamma$  the remaining computation can be done with a multiplication and an addition.

### 2.5 Dynamic Threshold

This technique, due to Morrin [12], combines edge emphasis with a dynamic threshold to produce a bilevel image from a continuous tone original. The description that follows conforms to the notation and conventions of this paper rather than the source paper. The most important change is that white and black are reversed in sense from that used in the Morrin paper.

For some point,  $I_{xy}$ , the decision to light point  $xy$  is made in two stages. First, the point is compared to two fixed thresholds:

$$\begin{aligned} \text{If } I_{xy} > A_{\max}, & \text{ then } P_{xy} = R; \\ \text{if } I_{xy} < A_{\min}, & \text{ then } P_{xy} = 0. \end{aligned} \quad (11)$$

If neither of the conditions is met,  $A_{\min} \leq I_{xy} \leq A_{\max}$ , and the full processing

algorithm is employed. The ambient or neighborhood average,  $B_0$ , is computed by a digital low-pass filter operating on the data ahead of  $I_{xy}$  in both the current and the previous scan line. The filter time constant was given as 8 pels. Concurrent with computing the ambient, a quantity, the composite difference,  $D_e$ , is calculated according to

$$D_e = \frac{I_{xy} - I_{x-1,y}}{2} + \frac{I_{xy} - I_{x,y-1}}{2}. \quad (12)$$

The ambient is scaled,

$$B_0' = \alpha B_0, \quad (13)$$

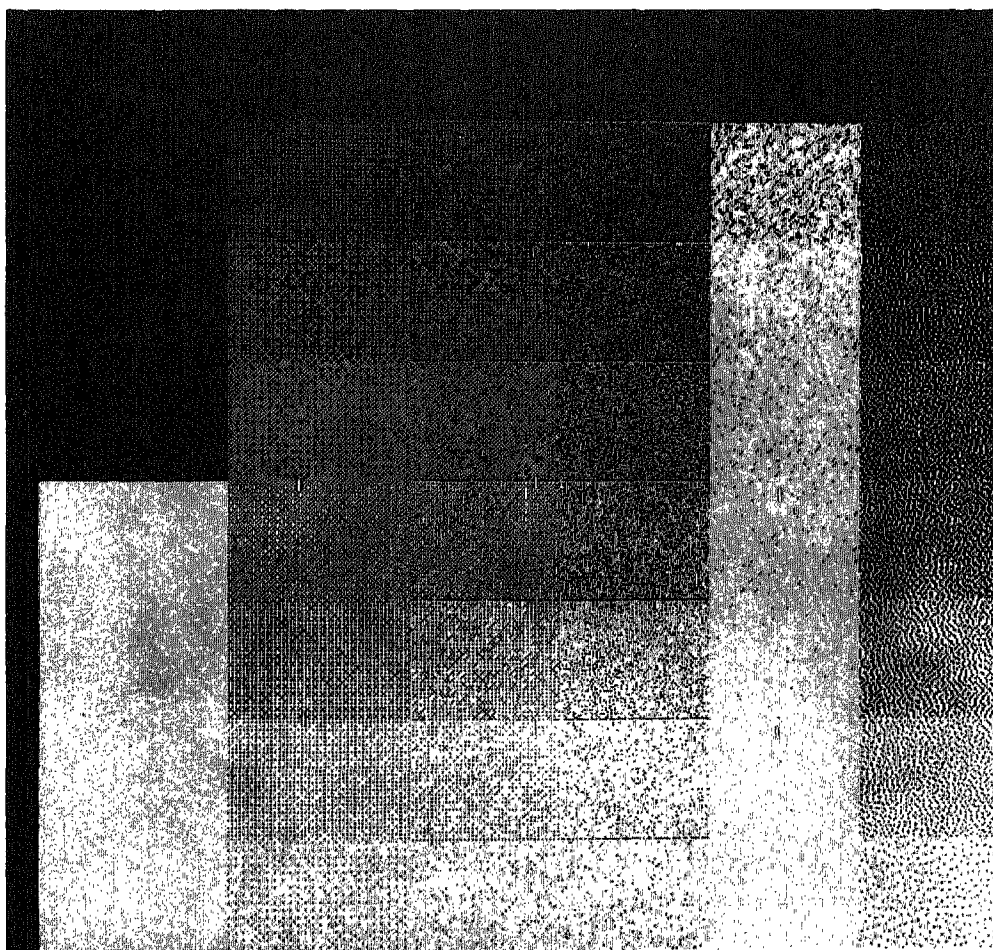


FIG. 31. A comparison of six different processing techniques. The horizontal bands are of constant intensity. The vertical bands represent the six techniques which are, from left to right, a fixed threshold of 127, ordered dither, constrained average with added dither, constrained average, dynamic threshold, and the minimized average error methods.

where  $\alpha < 1$  to bias the eventual decision toward the white region (on cells). Finally the decision is made:

$$\text{If } I_{xy} > mD_e + B_0', \quad \text{then } P_{xy} = R, \\ \text{else } P_{xy} = 0. \quad (14)$$

The quantity  $m$  is stated as an edge emphasis sensitivity coefficient and is given as  $-1$  in the source paper.

In assessing the operation of the algorithm the scaling operation, Eq. (13), with  $\alpha < 1$  is a much more important factor than indicated in the original paper. This scaling operation is essentially the same as the primary mechanism for reproducing the image gray scale in the constrained average algorithm. For the dynamic threshold algorithm,  $B_0' = B_0$  at the maximum black value,  $B = 0$ , while in the constrained average algorithm  $B_0' = B_0$  at the midpoint of the intensity range,  $R/2$ . Thus, the necessity of having a fixed threshold  $A_{\min}$  to force black regions is apparent, as the dynamic threshold is always less than the local average except at  $B = 0$ . Without the fixed threshold  $A_{\min}$ , about one-half the cells in the output could be expected to be lit in the darkest areas of the image. With  $m = -1$ , Eq. (14) can be rewritten as:

$$\text{If } I_{xy} > (I_{x-1,y} + I_{x,y-1})/2 + b_0'/2, \quad \text{then } P_{xy} = R, \\ \text{else } P_{xy} = 0. \quad (15)$$

In this case the resemblance to the constrained average algorithm is more apparent. The point intensity,  $I_{xy}$ , is being compared to a local average made up of one component subject to a constraint ( $b_0'/2$ ) and a component not so constrained. The resulting value is still a constrained neighborhood or local average and differs only in detail from the local average used in the constrained average algorithm.

Implementation, as in the constrained average process, requires two (or more) line memories to allow the neighborhood average to be computed. The exact number depends on the details of the neighborhood average calculation.

Figures 6, 19, 24, and 29 show processing by this algorithm with the parameters

$$A_{\min} = 40, \quad A_{\max} = 215, \quad \alpha = 0.96.$$

A wide range of parameters is possible. The value chosen for  $\alpha$  represents approximately the same compaction in the ambient as does  $\gamma = 10$  in Section 2.4.

## 2.6 Minimized Average Error

The display algorithm described in this section is predicated on choosing local patterns of lit cells in such a way as to minimize the intensity error between the source and displayed images. This technique has been described previously for a device capable of a small number (greater than two) of output levels [13]. A very similar technique, called error diffusion, has also been reported [17]. Qualitatively the techniques described in this section and the two references produce quite similar results.

The algorithm arises from the following considerations. At a point  $xy$  in the image there will be an error between the displayed intensity and the original

image as the original image contains more intensity levels than the displayed image

$$E_{xy} = I_{xy} - P_{xy}, \quad (16)$$

where  $E_{xy}$  is the intensity error at point  $xy$ ,  $P_{xy}$  is the displayed intensity, and  $I_{xy}$  is the original image intensity. The minimized average error approach is to choose successive  $P_{xy}$ 's in such a way as to minimize the accumulated error between the original and displayed images.

The algorithm is implemented as follows. A corrected intensity  $I'_{xy}$  is computed from the previously computed errors and the intensity,  $I_{xy}$ :

$$I'_{xy} = I_{xy} + (1/\sum_{ij} \alpha_{ij}) \sum_{ij} \alpha_{ij} E_{x+1,y+j}. \quad (17)$$

In this equation ranges of the indices  $i, j$  are defined by the definition of neighborhood of point  $I_{xy}$ . The matrix  $\alpha$  defines the relative contributions of the previously computed errors to the corrected intensity. The corrected intensity is compared to a fixed threshold,  $R/2$ , to determine whether the corresponding display element should be turned on:

$$\text{If } I'_{xy} > R/2, \text{ then } P_{xy} = R, \\ \text{else } P_{xy} = 0. \quad (18)$$

Finally, the error at point  $xy$ ,

$$E_{xy} = I'_{xy} - P_{xy}, \quad (19)$$

is computed and saved for use in generating succeeding  $I'_{xy}$  values.

The neighborhood of a point is defined by the matrix  $\alpha$  and for Figs. 7, 20, 25, and 30, the following matrix is used:

$$\alpha = \begin{vmatrix} 1 & 3 & 5 & 3 & 1 \\ 3 & 5 & 7 & 5 & 3 \\ 5 & 7 & * & - & - \end{vmatrix}. \quad (20)$$

The element marked \* is the position of the point  $I_{xy}$  under consideration and does not enter into the average error computation. Likewise, the elements marked— are ahead of the point  $xy$  in the scan line and no error values for these elements exist; consequently they cannot enter into the error computation.

The choice of matrix elements does not seem to change the general characteristics of the displayed image greatly, although there can be marked changes in the detailed, microscopic patterns observed. In general, as more elements are set to nonzero values the microscopic patterns tend to be smaller and more random appearing. Also, there is a strong correlation of on and off cells, which results in a picture containing very noticeable dot patterns that are artifacts of the processing and are not contained in the original image. The minimum size of the matrix needed to generate subjectively satisfactory results is probably about the size of (20).

As implemented, this algorithm requires three line memories to contain the successive error values. Also, a substantial number of computations for each pel is needed, as a weighted rather than a simple sum must be done. Boundary

handling consists of setting the error values to zero for a boundary two cells wide on each side and the top of the picture. Only the pels interior to this region are evaluated. The two-cell-width boundary is generally not noticeable in  $512 \times 512$  element pictures.

### 3. SIMULATION DETAILS

This section describes the computer simulation of the various algorithms described in Section 2. Data sources and processing and display equipment are described, and a discussion of the important aspects of the various algorithms is given.

#### 3.1 Data Sources

Three of the image files were obtained by scanning  $4'' \times 4''$  sections of photographic negatives on a Photomat P-1700 scanning microdensitometer. The scanning resulted in images quantized to eight bits on approximately an  $1800 \times 1800$  point matrix. The data were reduced to a  $512 \times 512$  sample size by choosing every third point of every third line. The amplitude of the data was scaled and normalized to span approximately 95% of the eight-bit (0-255) range accommodated in the data files.

The three files include a closeup of a face, a picture that has been heavily used in various picture processing studies. This picture is taken as representative of the needs of face-to-face visual communication. The second picture was copied from a technical magazine [14] and is considered representative of illustrative drawings often found in the technical literature. The third data file is three replicas of a paragraph of typed text. The center paragraph is the typewritten original, while the top and bottom are copies and have been tilted relative to the horizontal.

The fourth data file was generated by a program and was designed to allow a qualitative measure of the gray scale and line legibilities after processing by the various techniques. The contents of this image are described in Fig. 15. Also, a normal distribution random number generator was used to add a known amount of noise to the image data. Noise is required by the constrained average and dynamic threshold algorithms to generate a gray scale and the presence of signal noise generally allows a more meaningful comparison of the results of the processing.

#### 3.2 The Picture Processing Facility

All the processing, except the scanning of the test negatives, was done on a combined PDP-11/45 and PDP-11/20 system. The PDP-11/45 runs the UNIX [15] operating system and has sufficient computational, core, and disc resources to process and store all the data reported in this paper. The 11/20 is the controller in the Plasma Panel Display System (PPDS) [16] that is used to display the results of the processing operation. The two panels used in the PPDS are the Owens-Illinois 512-60 DIGIVUE panels providing  $512 \times 512$  cells at 60 cells

to the inch. All the processed pictures presented in this memorandum are photographs of one of the panels.

#### 4. DISCUSSION

The processed images presented generally illustrate the claims and discussions made in the sections describing the algorithm. However, some comparisons between the various algorithms should be made.

The control of the spatial frequencies of the intensity errors by the ordered-dither technique provides the best rendition of the tonal scale of the original images. This is very notable when dithered images are compared to the other processed images.

The second major result to note is that the edge emphasis techniques do make detail in the form of text and lines more visible. Compare the output of dither and the constrained average processing for the text and drawing images as an example of this. The length of the horizontal lines in the bottom quarter of the computer generated file (Figs. 26-30) gives an indication of the relative capabilities of the various processing techniques to render line structure visible.

As a final comparison, Fig. 31 was made to allow close comparison of the gray scale capabilities of the various techniques. The horizontal bands are of equally spaced intensities from 16 to 240, with added normally distributed noise. The vertical stripes are the result of processing the data with six differing techniques. Starting from the left these are: a fixed threshold of 127, ordered dither, constrained average with dither added to the signal, constrained average, the Morrin dynamic threshold technique, and the minimized average error process.

It is not the purpose of this paper to make a relative ranking of the various processing algorithms; however, it is clear that the ordered-dither technique is simultaneously simple to implement and capable of giving an excellent rendition to a large variety of subjects. Also, line and text detail in images can be made more visible by various edge emphasis techniques. Edge emphasis considerably complicates the implementation as some sort of local average must be computed on a point-by-point basis. The combination of edge emphasis and dither appears to be the best compromise technique for the pictures investigated.

#### ACKNOWLEDGMENTS

The authors thank J. O. Limb and C. S. Roberts for many helpful comments and discussions during the work reported on in this paper. The assistance of Helen Hanes in digitizing the negatives used as test data is also very much appreciated.

#### REFERENCES

1. S. Arnemann and M. Tasto, Generating halftone pictures on graphic terminals using run length coding, *Computer Graphics Image Processing* 2, 1973, 1-11.
2. K. Knowlton, and L. Harmon, Computer-produced grey scales, *Computer Graphics Image Processing* 1, 1972, 1-20.
3. W. D. Petty and H. G. Slottow, Multiple states and variable intensity in the plasma display panel, *IEEE Trans. Elect. Dev.* ED-18, 1971, 654-658.

4. K. Kurahashi, H. Tottori, F. Isogai, N. Tsuruta, Plasma display with gray scale, SID Symposium, Digest of Papers, 1973, 72-73.
5. S. Umeda, K. Murase, H. Ishizaki, K. Kurahashi, Picture display with gray scale in the plasma panel, SID Symposium, Digest of Papers, 1973, 70-71.
6. D. L. Fulton, A spatial gray scale for plasma display panels, SID Symposium, Digest of Papers, 1973, 20-21.
7. J. O. Limb, Design of dither waveforms for quantized visual signals, *Bell System Tech. J.* **48**, 1969, 2555-2582.
8. B. Lippel and M. Kurland, The effect of dither on luminance quantization of pictures, *IEEE Trans. Communication Technology* **6**, 1971, 879-888.
9. B. E. Bayer, An optimum method for two-level rendition of continuous-tone pictures, International Conference on Communications, Conference Record, 1973, (26-11)-(26-15).
10. C. N. Judice, J. F. Jarvis, and W. H. Ninke, Using ordered dither to display continuous tone pictures on an ac plasma panel, *Proc. SID*, Fourth Quarter (1974), 161-169.
11. J. F. Jarvis and C. S. Roberts, A new technique for the bilevel rendition of continuous tone pictures, *IEEE Trans. on Communications*, to be published.
12. T. H. Morrin, A black-white representation of a grey scale picture, *IEEE Trans. Computers* **C-23**, 1974, 184-186.
13. M. R. Schroeder, Images from computers, *IEEE Spectrum* **6**, 1969, 66-78.
14. *Bell Lab. Rec.* **51**, 1973, 328.
15. D. M. Ritchie and K. Thompson, The UNIX time sharing system, *Commun. ACM* **17**, 1974, 365-375.
16. J. F. Jarvis, A graphical display system utilizing plasma panels, *Computers and Graphics* **1**, 1975, 175-180.
17. R. Floyd and L. Steinberg, An adaptive algorithm for spatial grey scale, SID Symposium. Digest of Papers, 1975, 36-37.